2. Spinelli, H. J.; Harris, F. W. *Reactive Oligomers*; ACS Sym. Ser. 282, American Chemical Society: Washington DC, 1985.
3. Allen, G.; Bevington, J. C. *Comprehensive Polymer Science*; Pegamon Press: Oxford, 1989; Vol. 5, pp 499-532.
4. Kim, Y. S.; Kim, B. G.; Gong, M. S. *Polym. J.* **1994**, *26*, 1910.
5. Cho, H. G.; Kim, B. G.; Choi, S. H.; Gong, M. S. *Macromolecules* **1993**, *26*, 6654.
6. Robello, D. R.; Moore, J. A. *Macromolecules* **1989**, *22*, 1084.
7. Moon, H. S.; Kim, S. T.; Gong, M. S. *Makromol. Chem. Rapid Commun.* **1991**, *12*, 591.
8. Mehta, P. G.; Moore, J. A. *Macromolecules* **1993**, *26*, 916.
9. Mehta, P. G.; Kim, S. Y.; Moore, J. A. *Macromolecules* **1993**, *26*, 3504.
10. Moon, H. S.; Kim, J. S.; Kim, C. B.; Gong, M. S. *Polym. J.* **1993**, *25*, 193.
11. Shin, J. C.; Kim, T. M.; Gong, M. S. *Macromolecules* **1995**, *28*, 2212.
12. Ha, J. H.; Kim, C.; Gong, M. S. *Polym. J.* **1995**, *27*, 536.
13. Mikroyannidis, J. A. *J. Polym. Sci., Part A: Polym. Chem.* **1993**, *31*, 1771.
14. Li, H.; Hsu, K. Y.; Chang, T. C. *J. Polym. Sci., Part A: Polym. Chem.* **1991**, *29*, 1447.
15. Gong, M. S.; Park, W. S. *Macromol. Chem. Phys.* in press.

^{13}C NMR Studies of Metabolic Pathways Regulated by HSP104 in *Saccharomyces cerevisiae*

Kyunghee Lee*, Sooim Kang, and Susan Lindquist†

Department of Chemistry, Sejong University, Seoul 143-747, Korea
†Howard Hughes Medical Institute Research Laboratories, Department of Molecular Genetics and Cell Biology, The University of Chicago, Chicago, Illinois 60637, USA
Received September 22, 1997

HSP104 protein in *Saccharomyces cerevisiae* is known to provide thermotolerance when induced by various kinds of stresses, such as a mild heat shock, ethanol, and hypoxia. It helps cells survive at an otherwise lethal temperature. Mechanisms by which HSP104 protein works are yet to be elucidated. In order to understand a molecular basis of thermotolerance due to HSP104 protein induced by a mild heat shock, studies on respiratory pathways were carried out in the wild type as well as in the *hsp104* deleted mutant. Especially the degree of ^{13}C-acetate incorporation into glutamate-C4 was examined for both strains using ^{13}C-^{13}C homonuclear spin coupling measurements, since glutamate is in a rapid equilibrium with α-ketoglutarate in the TCA cycle. In addition, the temperature effects on the rate of ^{13}C incorporation are compared with or without HSP104 protein expressed. Finally, the inhibitory effect of HSP104 on the respiration pathway was confirmed by the measurements of oxygen consumption rates for both strains.

Introduction

HSP104 plays an important role in providing thermotolerance in *Saccharomyces cerevisiae*.[1] It helps cells survive short exposures to extreme temperatures. It is expressed at a basal level at a normal temperature (25 °C) and is very strongly induced at a moderate temperature (37 °C). It is also induced by a variety of other stresses, including ethanol, arsenate, and cadmium etc.[2]

It is not still clear how HSP104 makes cells resistant against extreme heat shocks. It has been a great concern to understand a molecular basis of HSP104 function in providing thermotolerance. It was demonstrated either by electron microscopy of whole cells or *in vitro* luciferase assay that HSP104 does not function as a molecular chaperone, but instead helps cells resolublize any aggregated proteins resulting from severe heat shocks.[3] Recently, it has drawn a great attention that transient overexpression of HSP104 protein can convert cells from [*PSI*$^+$] to [*psi*$^-$], which changes a translational fidelity.[4,5] Later [*PSI*$^+$] was confirmed to be a prionlike aggregate of the cellular protein Sup35, showing that [*PSI*$^+$] altered the conformational state of newly synthesized prion proteins.[6]

Another significant aspect of HSP104 is that the hsp104 gene has been highly conserved throughout evolution.[7] The Western and Northern blot analysis revealed that the expression of HSP104 protein and the production of corresponding mRNA were significantly elevated in several organisms when exposed to heat shocks.[7] It is highly homologous to the *E. coli* ClpA/ClpB family. The other heat-inducible members of this family are also present in bacteria, cyanobacteria, flagellated parasites and plants.[8]

Interestingly, the basal level of HSP104 is higher in yeast cells grown in acetate and galactose than in cells grown in

*To whom correspondence should be addressed.

glucose.[9] This implies that yeast cells express HSP104 mostly when they are in a respiratory metabolism, not in fermentative metabolism. This observation led us to investigate a possible effect of HSP104 protein on the respiratory pathway in yeast. In this paper, we looked at the efficiency of respiration in the presence or absence of HSP104 expressed by a mild heat pretreatment by ^{13}C NMR spectroscopy. We have exploited the significant information provided by the ^{13}C-^{13}C homonuclear spin couplings due to covalently bonded ^{13}C nuclei. In addition, as a final electron acceptor in the respiratory pathway, O_2 is presumably reduced to H_2O. Measurement of O_2 consumption in both strains will enlight the role of HSP104 in the respiration metabolism of yeast.

Results and Discussion

Detection of metabolites by ^{13}C NMR. In wild type cells, HSP104 was expressed at a basal level when grown at 25 °C in acetate medium, in which yeast cells must respire rather than ferment.[9] The existence of HSP104 in acetate was comfirmed by a western blotting in wild type cell extract.[9] In order to investigate any role of HSP104 on the respiratory pathway, both wild type cells and *hsp104* deleted mutant cells were grown to early log phase in rich media containing acetate. Natural abundant ^{13}C NMR spectra for wild type was obtained for perchloric acid extracts of yeast cells grown in the presence of acetate (Figure 1A). Since only very weak peaks were shown in the natural abundance spectrum, they were assigned with reference ^{13}C NMR spectra in which each metabolite was examined separately with respect to *p*-dioxane at 67.5 ppm. Weak signals at 27.8 ppm, 34.4 ppm, and 55.6 ppm were attributed to the C3, C4, C2 carbon atoms of glutamate, respectively.

^{13}C-acetate incorporation by ^{13}C NMR studies. As an effort to study metabolic thermotolerance in maize, Logan *et al.* have reported metabolic pathways examined by ^{13}C NMR spectroscopy of tissue extracts.[10] In corn, metabolism of glutamate and glutamine were markedly altered by heat shock according to the ^{13}C NMR spectra and enzymatic analysis. Changes in the incorporation of labeled precursors were investigated to confirm that the glutamate synthase activity in the mitochondria was changed in a fashion correlated with a level of protection against heat shock.[10] In this study the oxidation of ^{13}C-acetate in yeast was studied using ^{13}C NMR spectroscopy for the purpose of discovering a role of HSP104 protein in yeast respiration. ^{13}C NMR spectra were obtained for perchloric acid extracts of yeast cells grown in the presence of [2-^{13}C]acetate as a sole carbon source (Figure 1B). Cells grown to a log phase in acetate medium were resuspended in YPAc containing ^{13}C-acetate and incubated further for 30 min. ^{13}C-acetate is presumably incorporated into citrate, which in turn gets into α-ketoglutarate in the TCA cycle. Therefore data on ^{13}C enrichment of glutamate, which is in a rapid equilibrium with α-ketoglutarate,[11,12] were examined to quantify the incorporation of [2-^{13}C]acetate from ^{13}C NMR spectra. Compared to the spectrum of nonenriched extracts (Figure 1A), significant differences were found in the ^{13}C-enrichment levels of the glutamate-C2 and -C4 in Figure 1B. Patterns of resonance peaks in *hsp104* mutant were indistinguishable

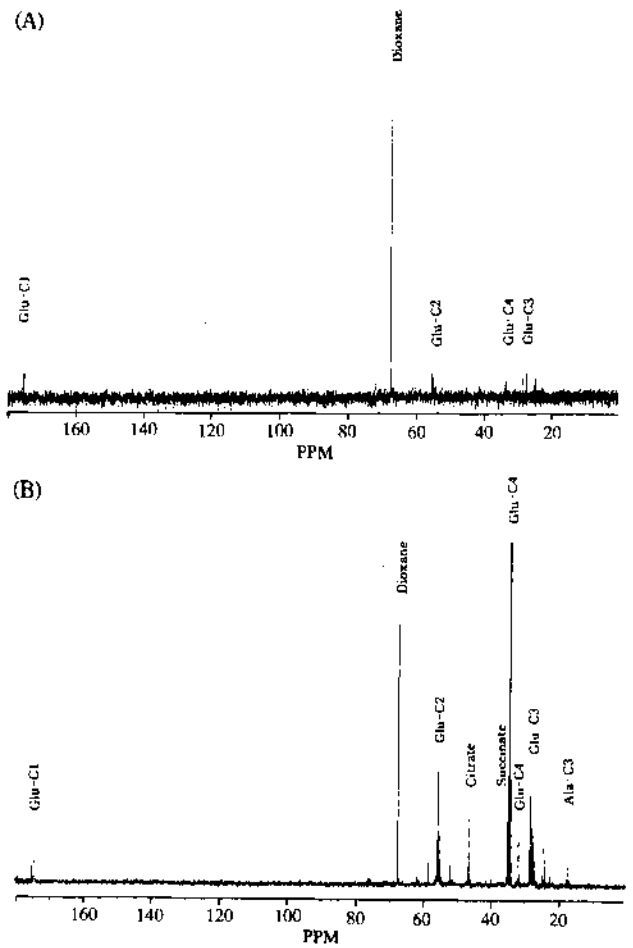

Figure 1. (A) Natural abundance ^{13}C NMR spectrum for wild type perchloric extract. Peaks were assigned by separate NMR experiments for each metabolite with respect to *p*-dioxane at 67.5 ppm. (B) ^{13}C NMR spectrum for perchloic acid extracts of yeast cells enriched by ^{13}C-acetate. Patterns of resonance peaks in *hsp 104* mutant were indistinguishable from those in wild type.

from those in wild type (data not shown). Resonances were assigned by comparison with spectra of standard solutions. Signals for the C2, C3, and C4 carbon of glutamate greatly increased compared with those in the natural abundance spectrum; An enhanced signal at 31.9 ppm was attributed to glutamine C4; Additional peaks were detected for alanine C 2 (17.5 ppm), acetate C2 (24.1 ppm), succinate C2 (35.1 ppm), citrate C2 (46.7 ppm), and asparagine C1 (52.1 ppm). These spectra were acquired under conditions that ensure equivalent peak intensities for all protonated carbon resonances within any given metabolites.

Interestingly it was observed that the glutamate-C4 peak at 34.4 ppm began to be split into a doublet as ^{13}C-acetate was incorporated (Figure 2). This observation was made due to ^{13}C-^{13}C homonuclear spin coupling, in which an isolated ^{13}C nucleus gives a various multiplet if attached to one or more ^{13}C nuclei. At the first turn of TCA cycle, condensation of [2-^{13}C]acetyl CoA with oxaloacetate would give rise to α-ketoglutarate and hence glutamate labelling only at C4. Cycling of α-[4-^{13}C]ketoglutarate through the TCA cycle would give rise to [2,4-^{13}C] and [3,4-^{13}C]glutamate and further cycling of the doubly enriched species

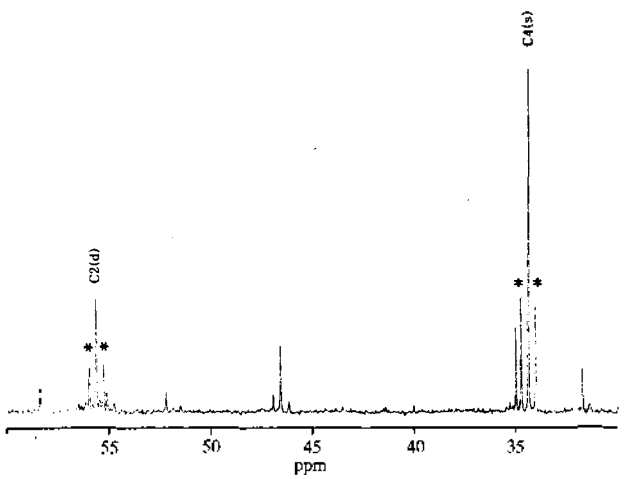

Figure 2. Splitting pattern of glutamate peaks. Peaks for glutamate-C2 and glutamate-C4 were split due to ^{13}C-^{13}C homonuclear spin coupling. The doublets are represented with (*).

would give rise successively to [2,4], [1,3,4] and [2,3,4]-, and thence to [2,4]-, [1,3,4]-, [2,3,4]- and [1,2,3,4-^{13}C]glutamate. [4-^{13}C]glutamate peak areas in spectra from extracts obtained from [2-^{13}C]acetate incubation were examined as an indicator of flux through the TCA cycle.[11] By intergrating the singlet and doublet peaks at the [4-^{13}C] and [2-^{13}C] glutamate, we were able to measure the relative turnover rate of TCA cycle (R) between the first turn and the second turn.

$$R = \frac{2nd\ turn}{1st\ turn} = \frac{[3,4\text{-}^{13}C]\ Glu}{[4\text{-}^{13}C]\ Glu} = \frac{C4(d)\text{–}C2(d)}{C4(s)\text{–}C2(s)}$$

Normalized by the number of yeast cells, each R value was found to be different between wild type and *hsp104* mutant (Figure 3). In the mutant, the ratio increased up to 70%

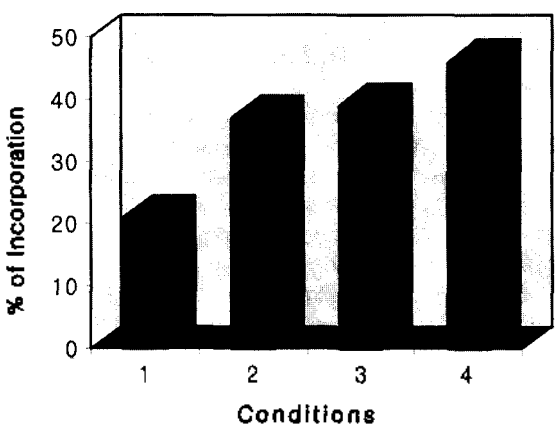

Figure 3. Incorporation of ^{13}C-acetate into glutamate-C4. The peaks for glutamate-C2 and C4 were integrated for a singlet and a doublet, respectively. A relative ratio (R) was normalized by the number of yeast cells, in which R is defined as a ratio between [C4(d)-C2(d)] and [C4(s)-C2(s)]. The extracts of wild type cells were examined for the relative incorporation efficiency after enriched by ^{13}C-acetate at 25 °C (condition 1) and 37 °C (condition 2). The similar observation was made for *hsp104* mutant grown in the presence of ^{13}C-acetate at 25 °C (condition 3) and 37 °C (condition 4).

compared to that of wild type. The higher rate of ^{13}C-incorporation observed at glutamate peaks implies that the rate of TCA cycle via α-ketoglutarate is faster in the *hsp104* mutant than in the wild type.

Effect of temperature on ^{13}C-acetate incorporation. In order to investigate an effect of temperature on ^{13}C-acetate incorporation, the extracts from both wild type and *hsp104* mutant were examined by ^{13}C NMR following incubation in the presence of [2-^{13}C]-acetate at 25 °C and 37 °C for 30 min, respectively. The ^{13}C-acetate incorporations were significantly enhanced when incubated at 37 °C for both strains (Figure 3), which suggests that either turnover rate of TCA cycle increases or cells lose the integrity of mitochondrial membrane at a high temperature. The difference of incorporations at two temperatures was found to be more significant in the wild type (70%) than in the mutant (20%). Perhaps because the mutant incubated at 25 °C behaves like the wild type grown at 37 °C, there is not as great a change in the mutant at 37 °C.

Determination of glutamate concentration. Branched from the TCA cycle, glutamate is rapidly formed from α-ketoglutarate. Therefore the level of glutamate in the cell extract can reflect the amount of α-ketoglutarate in the TCA cycle, thereby indicating the turnover rate of metabolites in the TCA cycle. Figure 4 shows the relative ratio of glutamate levels in the wild type and in the *hsp104* mutant at 25 °C, in which the mutant has about 2 fold amount of glutamte compared to the wild type. Similar difference was also shown at 37 °C when both strains were compared, which is in a good agreement with the NMR data (Figure 3).

O_2 consumption measurement. A proton leakage through the inner mitochonrial membrane has been observed as a result of a physiological phenomenon linked to the cold-sensitive phenotype in some yeast mutants.[13] It was also envisioned that the transfer of NADH and $FADH_2$ generated by coupling of the TCA cycle to the oxidative phosphorylation process might be altered in the case of *hsp104* mutant. Therefore oxygen consumption rates in both strains

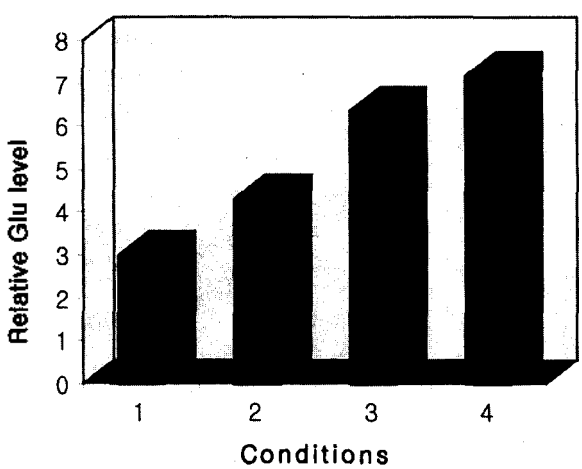

Figure 4. Glutamate concentrations. The level of glutamate was measured by the enzymatic method and compared for different conditions. Condition **1** and **2** are for the wild type extracts at 25 °C and 37 °C, respectively. Condition **3** and **4** are for the *hsp104* mutant extracts at 25 °C and 37 °C, respectively.

were investigated to check the possibility of blockade in the electron transfer or oxidative phosphorylation. A closed chamber which was saturated with oxygen was connected to an electrode to measure pO_2.[13] The oxygen pressure was monitored as a function of time and the oxygen concentration was calculated from the slope. A pattern of increase in the rate of oxygen consumption for the *hsp104* mutant was observed (Figure 5), consistent with the data of ^{13}C-acetate incorporation in ^{13}C NMR spectroscopy (Figure 3). We have no evidence for any direct role of HSP104 in the electron transport system, which connects the TCA cycle to O_2 consumption in the respiration pathway by transferring electrons. For this purpose, investigation of P/O ratios for two strains at various conditions are currently in progress using ^{13}P NMR spectroscopy in combination with O_2 consumption measurements. Our results, however, suggest a difference in the rate of carbon flux through the TCA cycle in wild type and *hsp104* mutant and a difference in the coupling of the TCA cycle to elctron transfer and oxidative phosphorylation.

Experimental

Strains. *S. cerevisiae* W303 (Mata *can1 his3 leu2 trp1 ura3 ade2*) and W304 (Mata *can1 his3 leu2 trp1 ura3 ade2 hsp104::LEU2*) were used.[1]

Preparation of ^{13}C-incorporated metabolites. Cells were grown in 1 L YPAc (10% yeast extract, 20% bacto-peptone, 0.05% sodium acetate) to an early log phase (~5×10^6 cells/mL) and harvested by centrifugation. The collected cells were resuspended in 200 mL of YPAc containing 2-^{13}C-sodium acetate at 0.5 g/liter. After 30 min incubation at different temperatures, cells were collected by rapid filtration to ensure fast harvest and complete removal of residual ^{13}C-acetate. Cells were extracted by adding 2 mL cold 6% perchloric acid ($HClO_4$) and vortexed at the setting of 10 for 30 sec ten times at 4 °C. After 1 hr precipitation, the unbroken cells were removed by centrifugation and the supernatant was neutralized by 3 M KOH. After another centrifugation, the supernatant was collected in a 15 mL tube and frozen immediately with liquid nitrogen. The lyophilized sample was dissolved in deuterated water (D_2O) containing Na_4EDTA and 2 μL/mL *p*-dioxane for NMR analysis.

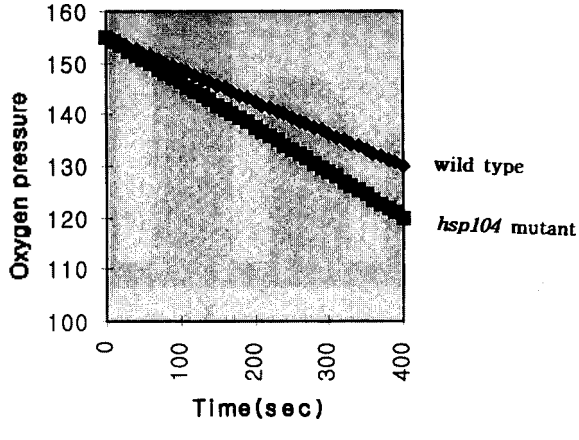

Figure 5. Oxygen consumption measurement. Using a Clark electrode, an amount of oxygen consumption in a closed chamber by cellular respiration was measured as a function of time.

^{13}C NMR spectroscopy. Proton-decoupled ^{13}C NMR spectra were recorded on a Bruker 200 NMR spectrometer operating at 4.7T. Data were acquired using a 60° carbon pulse and a 4.5s delay between pulses to ensure non-saturating conditions. The free induction decays were collected in 32 K of memory using consecutive blocks of 1000-2000 scans. Broad-band proton decoupling was employed using the WALTZ-16 sequence. A line broadening of 0.5-1.0 Hz was applied before Fourier transformation to improve the signal-to-noise ratio. All samples were maintained at 25 °C during data acquisition.

Determination of glutamate concentration. Glutamate concentration was measured by a conventional enzymatic method. Cell extracts were assayed for quantification of glutamate by monitoring conversion of α-ketoglutarate to glutamate by glutamate dehydrogenase.[13]

$$\alpha\text{-ketoglutarate} + NADH + NH_4^+ \longrightarrow \text{glutamate} + NAD^+ + H_2O$$

Oxygen Consumption Measurements. Rates of oxygen consumption for each strain in different conditions were measured using a Clark electrode[14] coupled to a biological oxygen monitor from Dr. Schumacker's laboratory (Univ. of Chicago). The amount of oxygen consumption in a closed chamber by cellular respiration was measured as a function of time. An oxygen consumption used for respiration was calculated from the resulting slope by a following equation.

$$O_2 \text{ concentration} = \text{slope} \times 0.08134 \times 60/ \text{ cell number in million } (\mu\text{mole/hr}/10^6 \text{ cells})$$

Acknowledgment. This work was supported partly by grants from the Korea Ministry of Education (BSRI-96-7403) and partly by Howard Hughes Medical Institute. Authors wish to thank Prof. D. Lynn for helpful discussion and critical advice throughout this study.

References

1. Sanchez, Y.; Lindquist, S. L. *Science* **1990**, *248*, 1112.
2. Parsell, D. A.; Taulien, J.; Lindquist, S. *Philosophical Transactions of the Royal Society of London. Series B: Biological Sciences* **1993**, *339*, 279.
3. Parsell, D. A.; Sanchez, Y.; Stitzel, J. D.; Lindquist, S. *Nature* **1991**, *353*, 270.
4. Chernoff, Y. O.; Lindquist, S. L.; Ono, B.; Inge-Vechtomov, S. G.; Liebman, S. W. *Science* **1995**, *268*, 880.
5. Lindquist, S.; Patino, M. M.; Chernoff, Y. O.; Kowal, A. S.; Singer, M. A.; Liebman, S. W.; Lee, K. H.; Blake, T. *Cold Spring Harbor Symposia on Quantitative Biology* **1995**, *60*, 451.
6. Patino, M. M.; Liu, J. J.; Glover, J. R.; Lindquist, S. *Science* **1996**, *273*, 622.
7. Parsell, D. A.; Kowal, A. S.; Singer, M. A.; Lindquist, S. *Nature* **1994**, *372*, 475.
8. Schirmer, E. C.; Glover, J. R.; Singer, M. A.; Lindquist, S. *Trends in Biochemical Sciences* **1996**, *21*, 289.
9. Sanchez, Y.; Taulien, J.; Borkovich, A.; Lindquist, S. *EMBO J.* **1992**, *11*, 2357.
10. Logan, T. M.; Zhong, P.; Lynn, D. G. *Biochemistry*

1992, *31*, 7256.
11. Dickinson, J. R.; Hewlins, M. J. E. *J. of General Microbiology* **1991**, *137*, 1033.
12. Small, W. C.; Brodeur, R. D.; Sandor, A.; Fedorova, N.; Guoya, L.; Butow, R. A.; Srere, P. A. *Biochemistry* **1995**, *34*, 5569.
13. Bergmeyer, H. U.; Graβl, M. *Methods of Enzymatic Analysis*; VCH Publishers: Deerfield Beach, U.S.A., 1985; p 20.
14. Manon, S.; Rakotomanana, F.; Guerin, M. *Eur. J. Biochem.* **1988**, *174*, 399.

Theoretical Study of the Nonlinear Optical Properties of Thiophene, Furan, Pyrrole, (1,2,4-triazole), (1,3,4-oxadiazole), and (1,3,4-thiadiazole) Monomers and Oligomers

U-Sung Choi*, Tae-Won Kim, Seung-Woo Jung, and Cheol-Ju Kim†

Department of Electronic Materials Engineering, Wonkwang University, Iksan 570-749, Korea
†Department of Chemistry, Chonbuk National University, Chonbuk 560-756, Korea
Received September 29, 1997

PM3 semiempirical calculations were carried out to study the frequency-dependent nonlinear optical properties of thiophene, furan, pyrrole, (1,2,4)-triazole, (1,3,4)-oxadiazole, and (1,3,4)-thiadiazole monomers and oligomers. The longitudinal component, α_{xx}, is the largest of three principle components. On the other hand, the out-of-plane component, α_{zz}, is the smallest. Moreover, the out-of-plane component (α_{zz}) of thiophene, furan, pyrrole, (1,2,4)-triazole, (1,3,4)-oxadiazole, and (1,3,4)-thiadiazole monomers show constant changes with increasing optical frequencies. The frequency-dependent first-order polarizabilities increase in the order: thiophene > (1,2,4)-triazole > pyrrole > furan > (1,3,4)-thiadiazole > (1,3,4)-oxa-diazole monomers and oligomers. The effects of $\beta(-2\omega;\omega,\omega)$ (SHG) shows a larger dispersion compared with $(-\omega;\omega,0)$(EOPE) and $\beta(0;-\omega,\omega)$ (OR). The second-order polarizabilities of thiophene, furan, pyrrole, (1,2,4)-triazole, (1,3,4)-thiadiazole, and (1, 3,4)-oxadiazole monomers for the various second-order effects have the order: $\beta(-2\omega;\omega,\omega)$ (SHG) > $\beta(-\omega;\omega,0)$ (EOPE) > $\beta(0;-\omega,\omega)$ (OR) and thiophene > pyrrole > (1,2,4)-triazole > furan > 1,3,4-thiadiazole > 1,3,4-oxadiazole monomers. The third-order polarizabilities for the various third-order effects have the following order: $\gamma(-3\omega;\omega',\omega,\omega)$ (THG) > $\gamma(-2\omega;0,\omega,\omega)$ (EFISHG) > $\gamma(-\omega;\omega',-\omega,\omega)$ (IDRI) > $\gamma(-\omega;0,0,\omega)$ (OKE). The effects of THG increase rapidly with increasing optical frequencies compared with the other effects. In particular, OKE effects increase most slowly with increasing optical frequencies. Also, the effects of THG for thiophene, furan, pyrrole, (1,2,4)-triazole, (1,3,4)-thiadiazole, and (1,3,4)-oxadiazole oligomers show the order thiophene > (1,2,4)-triazole > furan > pyrrole > (1,3,4)-thiadiazole > (1,3,4)-oxadiazole oligomers. In particular, the third-order polarizabilities of thiophene and (1,3,4)-thiadiazole oligomers are about four and three times larger than those of (1,3,4)-oxadiazole and (1,2,4)-triazole oligomer, respectively.

Introduction

Materials which exhibit highly nonlinear optical properties are essential for integrated optics, optical data processing, and photonic devices. In particular, organic materials with the large delocalization of the π electrons have been of great interest because they produce very large nonlinear responses.

Heterocyclic five-membered ring polymers(furan, pyrrole, thiophene, etc.) are the most extensively studied of the polyconjugated and conductive polymers.[1,2] Experimental measurements suggest that organic molecules containing heterocyclic rings (furan, pyrrole, thiophene) exhibit significant nonlinear optical properties. Theoretically and experimentally a new class of second-order nonlinear optical materials which utilize the coupling of electron-rich and electron-deficient aromatic heterocyclic units to provide the charge asymmetry for the nonlinear optical effect.[3]

A number of experimental observations of the nonlinear optical phenomena such as electrooptic Pockels effect (EOPE), second harmonic generation (SHG), optical rectification (OR), DC-electric field induced (EFI)SHG, third harmonic generation (THG), optical Kerr effect (OKE), DC-electric field induced(EFI)OR, etc. were reported for new materials with varied structures and dimensions.[4-8]

Keshari *et al.*[9] reported *ab initio* self-consistent-field calculations of linear and nonlinear polarizabilities of thiophene, furan, and pyrrole at their theoretically optimized geometries. Also, they reported the dispersion of $\alpha(-\omega;\omega)$ and those of $\beta(-2\omega;\omega,\omega)$ (SHG), $\beta(-\omega;\omega,0)$ (EOPE), $\beta(0;-\omega,\omega)$ (OR), $\gamma(-3\omega;\omega',\omega,\omega)$ (THG), $\gamma(-2\omega;0,\omega,\omega)$ (EFISHG), $\gamma(-\omega;\omega',-\omega,\omega)$ (IDRI), and $\gamma(-\omega;0,0,\omega)$ (OKE). Using an *ab initio* time-dependent coupled-perturbed Hartree-Fock method, the dispersion of linear and nonlinear optical pro-